In-Situ Measurement of Stresses in Carburized Gears via Neutron Diffraction

R.A. Le Master, B.L. Boggs, J.R. Bunn and J.V. Kolwyck

Management Summary

This paper presents the results of research directed at measuring the total stress in a pair of statically loaded and carburized spur gears. Measurements were made to examine the change in total stress as a function of externally applied load and depth below the surface. The measurements were made using the new Neutron Residual Stress Mapping Facility (NRSF2) instrument at Oak Ridge National Laboratory. A Static Load Application Device (SLAD) was developed to load the gear pair while mounted on the NRSF2 instrument. The paper includes a summary of various methods that are used to determine d_0 and a discussion of their applicability to carburized gears. The possibility of determining d_0 using ψ-tilt methods is discussed and results are presented for d_0 variation through the carburized layer determined using the $\sin^2\psi$ method.

Introduction

The total stress in an operating gear comprises two types: 1) externally induced stresses associated with the transmission of power, and 2) residual stresses associated with the heat treatment and machining of the tooth profiles. It is the combined effect of these two stress types that contributes to the life of a gear.

Stresses in metallic components can be measured using X-ray and neutron diffraction methods. Historically, these methods have been used to measure only residual stresses. X-ray and neutron diffraction methods involve measuring the interplanar spacing (d-spacing) of atoms in the crystal lattice using diffractometers that measure the position of the diffraction maxima, which is converted to d-spacing using Bragg's Law. The measured d-spacing is the average value for a group of grains suitably oriented within an irradiated surface area or volume. The change in d-spacing between stressed and unstressed states allows the determination of strains and, consequently, stresses.

In recent years, there has been interest in using neutron diffraction methods to measure the in-situ stresses in operating equipment. It is hypothesized that the penetrating feature of neutrons will allow the measurement of operating stresses inside mechanical components—which would not be possible via X-ray methods. A specific goal of this research was to determine the degree to which neutron diffraction can be used to measure the total stress in meshed carburized gears that are under static load. Considering statically-loaded-but-meshed gears as a first step would allow the effects of the near-surface chemistry, phases and microstructures to be isolated from dynamically induced phenomena.

Neutron Diffraction

Neutron diffraction is an experimental method used to study the structure of crystalline materials. Neutron diffraction instruments include a source capable of generating a stream of neutrons, or beam. This beam is directed at a sample, and the intensity of the scattered neutrons is measured using detectors. Variations of the intensity at different angular positions around the sample provide information about its crystal structure.

There are two primary types of neutron sources—nuclear reactors and spallation. The research presented in this report was conducted using the NRSF2 instrument that receives neutrons from the High-Flux Isotope Reactor (HIFR). HIFR is located at the Oak Ridge National Laboratory in Oak Ridge, TN.

Figure 1 presents a schematic of the NRSF2 instrument that traces the neutron beam from the reactor to the six position-sensitive detectors (PSDs). The beam leaving the reactor core contains many wavelengths, and a deformable Si crystal monochromator is used to obtain one of six possible wavelengths. A wavelength of 1.54 angstroms associated with the Si 422 plane was used for most of this research.

The single wavelength beam leaving the monochromator passes through a snout containing slits. The slits create a rectangular opening that control the incident beam width and height. The beam leaving the slits passes through the sample

that diffracts a fraction of the incident neutrons. When the beam encounters grains within the sample that have their lattice planes oriented in a particular direction, the beam will diffract and cause a peak in the measured intensity.

The scattering angle at which the peak will occur is governed by Bragg's Law:

$$\lambda = 2d \sin \theta \qquad (1)$$

where λ is the wavelength of the incident beam measured in angstroms, d is the lattice spacing between the atoms in the diffracting plane measured in angstroms, and θ is the diffraction angle (Figs. 2 and 3) in either degrees or radians. The d-spacing is obtained by rewriting Equation 1 as:

$$d = \frac{\lambda}{2 \sin \theta} \qquad (2)$$

The diffraction angle is determined by fitting a curve to the detector intensity data. The location of the peak intensity defines the diffraction angle. The wavelength of the radiation leaving the monochromator enables the calculation of the d-spacing using Equation 2.

In-Situ Strain Measurement

Static load application device (SLAD). SLAD was designed to hold and statically load the two gears used in these experiments. SLAD was also designed to be compatible with the NRSF2 instrument. The SLAD contains two major sub-assemblies—1) a loading fixture (Figs. 2a and 2b) and 2) a pump sub-assembly (Fig. 3). The two sub-assemblies are connected by a 10-foot-long hydraulic hose. A static torque is applied to the test gear using a hydraulic cylinder. This torque is transferred from the test gear to a mating gear that is prevented from rotating by a single tooth rack. The orientation of the test gear in the SLAD was designed so that the principal direction of the bending stress at the critical cross section was horizontal. This enabled the alignment of SLAD with the incident and diffracted beams that also lie in the horizontal plane. The gears are also positioned so that the contact point is at the worst load radius.

SLAD was designed to induce a 140 ksi bending stress at the critical cross section in the fillet region of the tooth. By using the equations at the bottom of Table 1, it was determined that this stress occurs at a hydraulic cylinder pressure of approximately 1,400 psi. The bending stress and associated strain for each of the pressures used in the tests are shown in Table 1. The 140 ksi- maximum stress level was chosen because the compressive, residual stresses of this magnitude— measured on the surface of the gears using x-ray diffraction (Ref. 1)—would be approximately balanced out and the resulting stress would be near zero.

Experimental setup. The experiment was designed to measure d-spacing in three orthogonal directions using the SLAD and NRSF2 instruments. The measurement of d-spacing in three orthogonal directions required mounting the
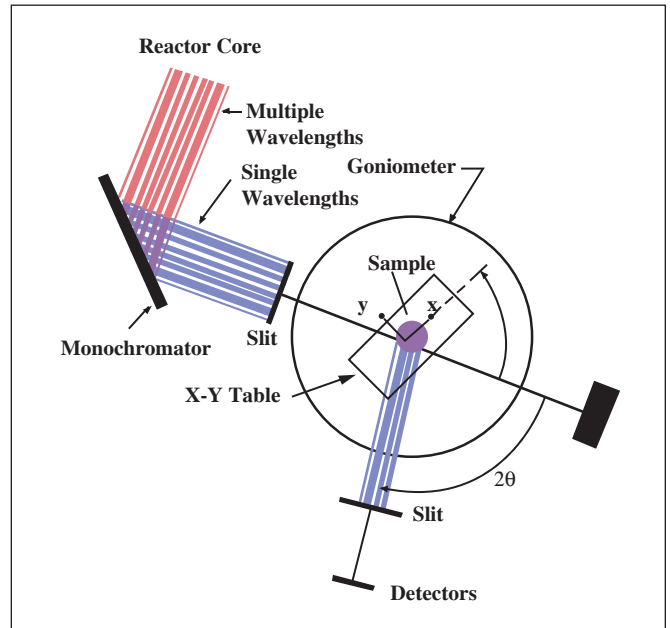
Figure 1—NRSF2 neutron beam schematic.

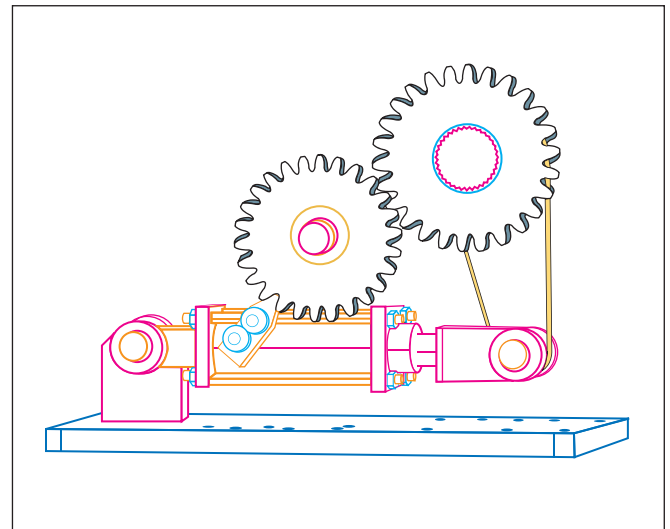Figure 2a—SLAD load fixture showing the two mating gears.

Figure 2b—CAD rendering of SLAD showing the hydraulic cylinder and torque arm used to load the gears.

Figure 3—Manually operational hydraulic pump used to load gears (plastic container is for spill containment).

Table 1—Critical bending stress and strain.

Cylinder pressure, psi	Torque, in-lb	Transverse tooth force, W_t, lb	Peak bending stress, σ_b	Peak bending strain ε_b
116	2,640	845	11.9	410
340	7,740	2,480	34.8	1,200
625	14,200	4,540	63.7	2,200
883	20,100	6,430	90.2	3,110
1,136	25,900	8,290	116.0	4,000
1,387	31,600	10,100	142.0	4,900

$$\sigma_b = \frac{W_t\,P_d}{F\,J}$$

$$\varepsilon_b = \frac{\sigma_b}{E}$$

$J = 0.38$
$F = 0.75$ in;
$P_d = 4$ teeth/in
$E = 29 \times 10^6$ psi

Table 2—D-spacing for longitudinal strain component vs. measurement depth and hydraulic cylinder pressure.

Depth, mm	Average pressure, psi					
	116	340	625	883	1136	1387
	d-spacing (A)					
0.08	1.16925	1.17093	1.17111	1.17231	1.17246	1.17280
0.25	1.16997	1.17040	1.17228	1.17245	1.17320	1.17298
0.50	1.17052	1.17157	1.17190	1.17272	1.17273	1.17287
0.75	1.17081	1.17182	1.17262	1.17239	1.17256	1.17289
1.00	1.17106	1.17193	1.17196	1.17249	1.17251	1.17299
1.25	1.17113	1.17196	1.17223	1.17251	1.17298	1.17297
1.50	1.17138	1.17181	1.17211	1.17257	1.17280	1.17278
1.75	1.17156	1.17192	1.17218	1.17249	1.17279	1.17283
2.00	1.17169	1.17218	1.17225	1.17252	1.17233	1.17271

Table 3—D-spacing for lateral strain component vs. measurement depth and hydraulic cylinder pressure.

Depth, mm	Average pressure, psi					
	119	363	619	894	1125	1389
	d-spacing (A)					
0.08	1.17063	1.17078	1.17097	1.17092	1.17118	1.17171
0.25	1.17118	1.17082	1.17102	1.17131	1.17103	1.17107
0.50	1.17132	1.17131	1.17105	1.17090	1.17085	1.17102
0.75	1.17132	1.17117	1.17112	1.17117	1.17101	1.17106
1.00	1.17145	1.17121	1.17136	1.17135	1.17134	1.17129
1.25	1.17140	1.17164	1.17164	1.17158	1.17154	1.17155
1.50	1.17182	1.17168	1.17171	1.17172	1.17168	1.17163
1.75	1.17169	1.17178	1.17166	1.17163	1.17163	1.17158
2.00	1.17170	1.17170	1.17163	1.17155	1.17160	1.17153

Table 4—D-spacing for normal strain component vs. measurement depth and hydraulic cylinder pressure.						
Depth, mm	Average pressure, psi					
	104	359	614	868	1182	1352
	d-spacing (A)					
0.00	1.17264	1.16929	1.16903	1.16903	1.1927	1.16905
0.25	1.17195	1.16920	1.16900	1.16900	1.16953	1.16891
0.50	1.17196	1.16929	1.16899	1.16889	1.16947	1.16925
0.75	1.17205	1.16905	1.16892	1.16892	1.16941	1.16923
1.00	1.17178	1.16944	1.16903	1.16903	1.16975	1.16931
1.25	1.17178	1.16893	1.16921	1.16921	1.16955	1.16918
1.50	1.17185	1.16916	1.16925	1.16925	1.16969	1.16925
1.75	1.17146	1.16914	1.16935	1.16935	1.16957	1.16925
2.00	1.17183	1.16917	1.16943	1.16943	1.16958	1.16934

SLAD on the NRSF2 instrument in three orientations.

- The first orientation was chosen to measure the d-spacing for the longitudinal strain component at the location of the critical bending stress in the fillet area. A 3 × 0.3 × 3 mm slit arrangement was used.
- The second orientation was achieved by rotating the Ω-axis of the NRSF2 instrument by 90°. This orientation was used to measure the d-spacing for the lateral strain component at the critical bending stress location. The same slit arrangement was used.
- The third orientation was orthogonal to the first two orientations and was achieved by physically rotating the SLAD by 90°. This orientation was used to measure the d-spacing for the normal strain component at the bending stress location. A "hanging slit" configuration was required with the lateral and normal directions to avoid interference issues between the NRSF2 instrument and the SLAD.

The d-spacing measurements were taken at nine depths—0.08; 0.25; 0.50; 0.75; 1.00; 1.25; 1.50; 1.75; and 2.00 mm—in each orientation, and at six hydraulic cylinder pressures of approximately 100; 360; 620; 880; 1,140; and 1,400 psi. The actual pressures used in each orientation were slightly different due to the inability to achieve a precise pressure using the manually operated pump.

Experimental data. Measured d-spacing for the longitudinal, lateral and normal directions at various pressures and depths is summarized in Tables 2, 3 and 4. All of the measurements were taken near the center of the tooth (8.5 mm in from the side of the gear). Figures 4, 5, and 6 show all of the d-spacing for a particular direction versus depth on a single graph.

SLAD data analysis. The effect of increasing the tooth load by an external source on d-spacing for the longitudinal strain component is clearly seen in Figure 4. At the lowest load level (116 psi cylinder pressure), the presence of the compressive residual stress state is evident. The d-spacing is smallest near the surface where the compressive residual stress is highest. The d-spacing increases as the measurement depth
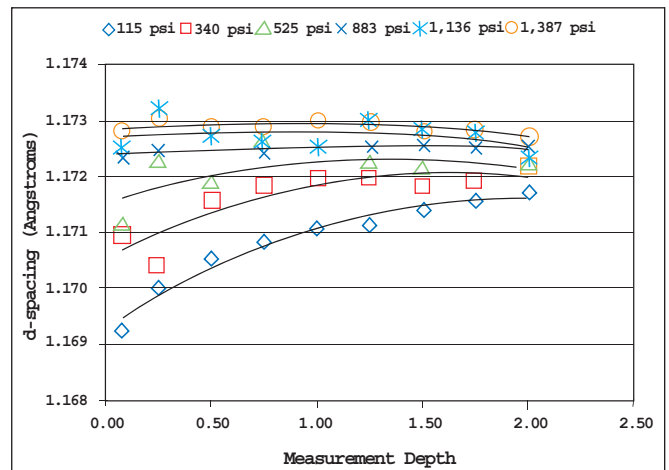

Figure 4—Variation of d-spacing for the longitudinal strain component with depth at different test pressures.

inside the carburized layer increases. This corresponds to a decreasing compressive stress state with increasing distance from the surface. As the tooth load is increased, the d-spacing increases—which is expected from the combination of a compressive residual stress and tensile stress resulting from the external load.

The SLAD device was designed to create a total stress of zero at the critical stress location on the fillet, at a pressure of 1,400 psi. The data shown in Figure 4 suggests that this was accomplished. At 116 psi, the compressive d-spacing gradient is clearly seen. In contrast—at a hydraulic cylinder pressure of 1,387 psi—the d-spacing gradient is nearly zero. The canceling of the d-spacing gradient as the cylinder pressure is increased is consistent with the compressive residual stress on the surface of 140 ksi, as measured using x-ray diffraction. It also shows that the AGMA tooth-bending equation given as,

$$\sigma = \frac{W_t P_t}{FJ} \qquad (3)$$

where W_t is the transverse component of the contact force, P_d is the diametral pitch, F is the face width, and J is the bending geometry factor (0.38 for the gears used in this test), gave accurate results. Further increases in hydraulic cylinder
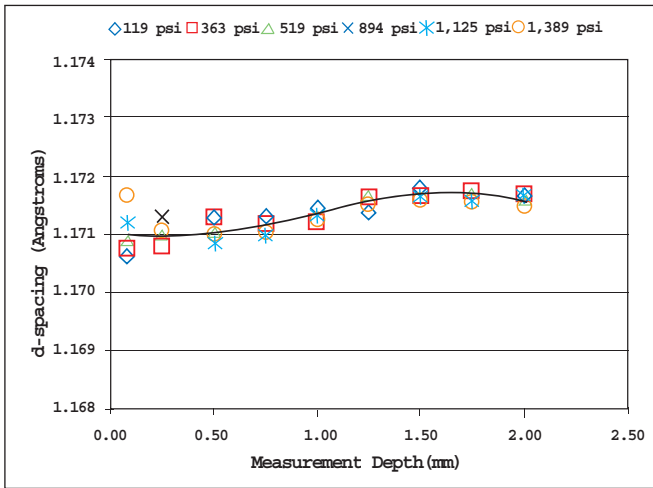
Figure 5—Variation of d-spacing for the lateral strain component, with depth at different test pressures.
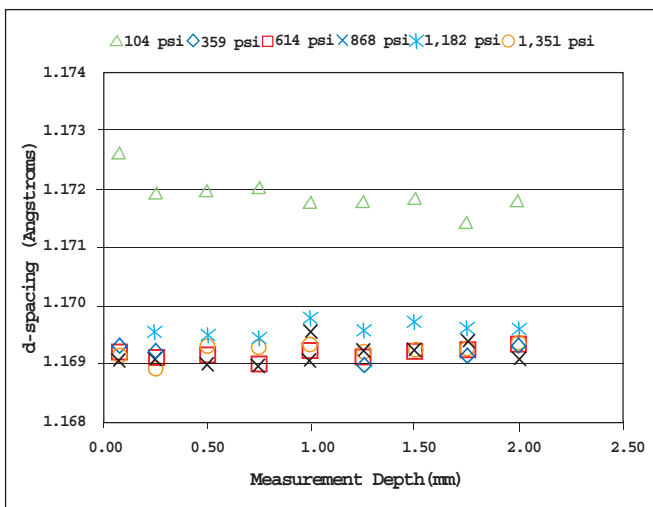

Figure 6—Variation of d-spacing for the normal strain component, with depth at different test pressures.

pressure result in higher d-spacing on the surface.

The effect of increasing tooth load on the d-spacing for the lateral strain components is not pronounced. The d-spacing data for the lateral direction is nearly the same for all pressures, and a single line can be fit to all of the data (Fig. 5). The measurements for all three strain components were made on a plane parallel to the sides of the gear and bisecting the center of the gear teeth. This plane is a plane of symmetry for the lateral direction and a state of plane strain exists. This condition leads to the lateral strains being zero for all pressures. At the location where the measurements were made, the total stresses (residual and externally induced) depend only on the residual stresses. This would not be expected if measurements were made off of the plane of symmetry. As one moves farther away from the plane of symmetry—i.e., closer to either side—it is expected that a condition approaching plane stress would be observed. This variation in the lateral strain/stress component across the width of a tooth is seen in finite element analyses.

There was no effect of increasing the tooth load on the d-spacing for the normal strain component (Fig. 6). All of the data can be fit closely with a single—almost horizontal—line.

One data set is offset from the others. This offset is thought to be due to possible movement of one of the hanging slits. The normal stress component is zero at the surface, and one would expect that the normal strain component would be a function only of Poisson ratio effects. The d-spacing for the normal strain component was not expected to change much, but it was expected that Poisson ratio effects would show a scaled variation of the data from the longitudinal direction.

Strain calculations. The calculation of strains using d-spacing data is accomplished using the equation:

$$\varepsilon = \frac{d-d_0}{d_0} \tag{4}$$

where d is the d-spacing measured in one of three mutually orthogonal directions, and d_0 is the strain-free d-spacing. Carbon, phase and microstructure gradients within the carburized surface layer will cause d_0 to vary through the thickness. As pointed out by Withers (Ref. 2), "Even slight changes in composition can bring about large changes in lattice spacing." Withers also discusses a variety of methods that can be used to determine d_0. These include powders, cubes, combs and $\sin^2\psi$ methods.

The measurement of d_0 and its variation within the carburized layer is not trivial. Two attempts to measure the variation of d_0 in the carburized layer using $\sin^2\psi$ methods are documented in Reference 3. In both cases, the measurements were inconsistent and confidence in the d_0 results was low. Another attempt to measure the variation of d_0 in a carburized layer by other methods was also unsuccessful (Ref. 4). Since we were unsuccessful in measuring d_0, no computed strain results are reported.

Stress calculations. Although strains were not computed due to the inability to determine d_0, the method by which stresses could be computed is presented for completeness. The conversion of strains to stresses requires a constitutive equation that relates stress to strain. The material in the core of the gear (outside of the carburized region) can be described as a homogeneous, isotropic material. However, the material *within* the carburized region is not homogeneous and the degree of isotropy is unknown. The macroscopic properties (Young's modulus, E, and Poisson's ratio, v) of hardened, high-carbon steel are close to those of a low-carbon, unhardened steel. Therefore, it is reasonable to assume that even though the material in the carburized region is not homogeneous at the microscopic scale, the macroscopic properties E and v do not vary significantly.

The form of the constitutive equation for either an isotropic or orthotropic material is shown as

$$
\begin{Bmatrix} \sigma_{11} \\ \sigma_{22} \\ \sigma_{33} \\ \sigma_{12} \\ \sigma_{23} \\ \sigma_{13} \end{Bmatrix} =
\begin{bmatrix}
C_{1111} & C_{1122} & C_{1133} & 0 & 0 & 0 \\
C_{1122} & C_{2222} & C_{2233} & 0 & 0 & 0 \\
C_{1133} & C_{2233} & C_{3333} & 0 & 0 & 0 \\
0 & 0 & 0 & C_{1212} & 0 & 0 \\
0 & 0 & 0 & 0 & C_{2323} & 0 \\
0 & 0 & 0 & 0 & 0 & C_{1313}
\end{bmatrix}
\begin{Bmatrix} \varepsilon_{11} \\ \varepsilon_{22} \\ \varepsilon_{33} \\ \varepsilon_{12} \\ \varepsilon_{23} \\ \varepsilon_{13} \end{Bmatrix} \tag{5}
$$

This equation shows no coupling between the normal and shear strains. Since neither the degree of isotropy nor the orthotropic material constants are known, the equations for an isotropic material would normally be used to convert the measured strains to stresses. Equation 5 can be simplified to Equation 6 if only stresses normal to the orthogonal surfaces are of interest. This equation is not limited to principal strain or stress components, and can be used for any set of orthogonal stresses and strains.

$$\begin{Bmatrix} \sigma_{11} \\ \sigma_{22} \\ \sigma_{33} \end{Bmatrix} = \begin{bmatrix} C_{1111} & C_{1122} & C_{1133} \\ C_{1122} & C_{2222} & C_{2233} \\ C_{1133} & C_{2233} & C_{3333} \end{bmatrix} \begin{Bmatrix} \varepsilon_{11} \\ \varepsilon_{22} \\ \varepsilon_{33} \end{Bmatrix} \tag{6}$$

Design and neutron diffraction experimental issues. Most of the challenges faced in using SLAD were associated with avoiding interferences with the NRSF2 instrument. Several iterations were made during the design of SLAD to minimize beam attenuation. Windows were cut and bearing mounting plates were moved to achieve the best design. Future attempts at in-situ measurements of total stresses should consider the design of slit-mounting hardware that is specific to the loading device.

An accumulator should also be incorporated into the hydraulic loading system to enable more precise load control and to eliminate drift in hydraulic pressure over time. During the experiments, the pressures were observed to drift by as much as ± 3% during the five- to six-hour data acquisition period. On occasion, the variation in pressure was observed to follow temperature changes in the HIFR beam room. At higher cylinder pressures, the pressure is thought to have decreased slightly due to relaxation of the stresses in the many tapped holes in the aluminum plates making up the SLAD.

Conclusions

The primary objective was to measure the total stress in a pair of statically loaded, carburized gears. The total stresses comprise both residual stresses and those due to the external loading. SLAD was designed to load two carburized spur gears while positioned in the NRSF2 instrument. SLAD and the NRSF2 were successfully used to measure the d-spacing at various depths and tooth loads. The d-spacing data very clearly shows the change in d-spacing as a function of depth and pressure for the longitudinal strain component. The d-spacing at low tooth loads shows characteristics consistent with a compressive, residual stress state. Increasing the tooth load created tensile stresses that negated the effects of the residual stress. The d-spacing associated with the lateral and normal strain components was not sensitive to a change in tooth load. This result would not be expected for d-spacing associated with the lateral strain component at points off the plane of symmetry that were used in this experiment.

Attempts to measure the variation of the strain-free d-spacing (d_0) using the $\sin^2\psi$ method were unsuccessful and prevented the calculation of strains and stresses from the

d-spacing data.

The SLAD experiments demonstrated the ability to measure the change in total d-spacing resulting from residual and externally induced stresses using neutron diffraction. The near- surface d-spacing data obtained from the NRSF2 and SLAD was consistent with x-ray diffraction data. The data also was consistent with the AGMA bending stress equation that was used during the design of the SLAD.

References
1. LeMaster, R.A, B.L. Boggs, J.R. Bunn, C.R. Hubbard and T. Watkins. "Grinding-Induced Changes in Residual Stresses of Carburized Gears," AGMA Fall Technical Meeting, Detroit, MI, October, 2007. (Also appeared in the March/April 2009 issue of *Gear Technology*.)
2. Withers, P.J., M. Preuss, A. Steuwer and J.W.L. Pang. "Methods for Obtaining the Strain-Free Lattice Parameter when using Diffraction to Determine Residual Stress," *Journal of Applied Crystallography*, 40, 2007, 891–904.
3. LeMaster, R.A., B.L. Boggs, J.R. Bunn, J.V. Kolwyck, C.R. Hubbard and W.B. Bailey. "In-Situ Measurement of Stresses in Carburized Gears via Neutron Diffraction," Report to the American Gear Manufacturers Association Foundation, March, 2008.
4. Bourke, M.A.M., P. Rangaswamy, T.M. Holden and R. Leachman. "Complementary X-Ray and Neutron Strain Measurements of a Carburized Surface," *Materials Science and Engineering,* A 257, 1998, 333–340.

Bryan Boggs *in 2007 received a bachelor's degree in engineering with a specialty in mechanical engineering from the University of Tennessee at Martin. He was the recipient of the Outstanding Upper Division Engineering Student Award at UT Martin in 2007.*

Jeffrey Bunn *graduated from the University of Tennessee at Martin with a bachelor's degree in engineering and a concentration in civil engineering in May 2007. He is currently a doctoral student in the civil engineering department at the University of Tennessee Knoxville. His research is in the pairing of neutron diffraction and neutron imaging techniques to characterize hydrogen fuel cells. He is an IGERT fellow on the STAIR (Sustainable Technology through Advanced Interdisciplinary Research) program at UT Knoxville.*

Dr. Robert Le Master *is a professor in the department of engineering at the University of Tennessee at Martin, where he teaches courses in the general areas of machine design and materials science. His research interests lie in carburization processes and associated residual stresses. Prior to entering academia, he worked in the aerospace industry, where he contributed to NASA and U.S. Air Force projects. He is the recipient of the Stanley Jones Professorship at UT Martin and is the recipient of several teaching awards.*